

## CHAPTER II

### LITERATURE REVIEW

#### 2.1. Theoretical Background

##### 2.1.1 Theoretical of Gas Transport in Membranes

Membranes are semi-permeable barriers which enable to separate substances by various mechanisms such as solution/diffusion, adsorption/diffusion and molecular sieve. Three types of membranes are organic polymer membranes, inorganic membranes and mixed matrix membranes and can be porous to non-porous. A membrane is a device that permits the separation of one or more materials from a liquid or gas mixture on the basis of their diffusion rates through the membrane materials. In general, the rate at which a particular gas will move through the membrane can be determined by the size of the molecule, the concentration of gas, the pressure difference across the membrane and the affinity of the gas to the membrane material. The two main parameters defining membrane performance are permeability and selectivity. There are five possible mechanisms for membrane separation (Olajire, 2010).

For porous membranes:

- (1) Knudsen diffusion: the gas components are separated based on the differences in the mean free path of the gas molecules.
- (2) Molecular sieving: the gas components are separated based on size exclusion, the size being the kinetic diameter of the gas molecules.
- (3) Surface diffusion: the gas molecules with higher polarity are selectively adsorbed onto the surface of the membrane and pass through the membrane by moving from one adsorption side to another side.
- (4) Capillary condensation: capillary condensation occurs when the pore size and the interactions of the penetrant with the pore walls cause condensation in the pore that influences the rate of diffusion across the membrane (Lee and Hwang, 1986).

Gas molecules are transported through a porous inorganic membrane by these four main transport mechanisms.

For dense membranes:

(5) Solution-diffusion: the gases are separated by their solubility within the membrane and their diffusions through the dense membrane matrix. This is the usual separation mechanism for polymeric membranes e.g., rubbers, polyimides, and cellulose acetate.

Gas molecules transport through a polymeric membrane by a solution-diffusion mechanism, a molecular sieve effect and Knudsen diffusion (Powell and Qiao, 2006). However, the most common mechanisms are molecular sieving and solution-diffusion occurring in the polymeric membranes.

For mixed matrix membranes, to properly choose the dispersed and continuous phases, one must take the transport mechanisms and the gas component preferentially transporting through the membrane into consideration. In some cases, it is more sensible to allow the smaller component to pass through; therefore, inorganic fillers with molecular sieving characteristics and polymers based on the size selection should be combined to produce MMMs. On the other hand, the selective transport of more condensable molecules through the membrane is more economical in some industrial applications. To fulfill this target, the MMMs may include microporous media that favor a selective surface flow mechanism and polymers that separate the mixtures by solubility selectivity. The MMMs thus produced enable the selective adsorption and/or surface diffusion of more condensable component, while excluding the less condensable component (Chung *et al.*, 2007).

### 2.1.2 Polymeric Membranes

Polymeric membrane is widely used due to its relatively easy to manufacture and is suitable for low temperature applications. There are three types of polymeric membrane based on mechanism of gas separation. First, a porous membrane uses molecular sieve to separate one type of molecules from other molecules by using diffusion mechanism. While passing through porous membrane with gases, the smaller molecules can diffuse into pores of membrane and pass

through a permeate side. For the bigger molecules, they can diffuse down into pores of membrane and cannot pass through a permeate side, but they are rejected and stay at a retentate side of the membrane. The molecular sieving mechanism is shown in Figure 2.1.

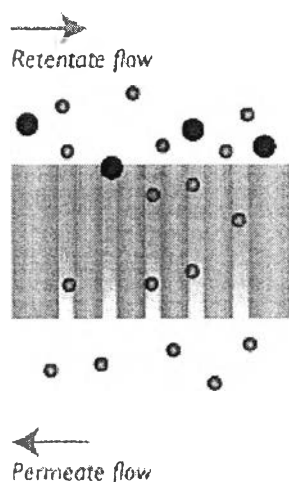


**Figure 2.1** The molecular sieving mechanism for a porous membrane ([www.co2crc.com.au/aboutccs/cap membranes.html](http://www.co2crc.com.au/aboutccs/cap%20membranes.html)).

The second type of the polymeric membrane is nonporous membrane or dense membrane by using the difference in solution-diffusion of molecule. There are three steps in solution-diffusion mechanism for dense membrane: (1) adsorption or absorption upon the upstream boundary, (2) diffusion through the polymeric membrane, (3) desorption or dissolution at the opposite interface of the membrane. This solution-diffusion mechanism is driven by a difference in thermodynamic activity between the interface of upstream and downstream. The solution-diffusion mechanism is shown in Figure 2.2.

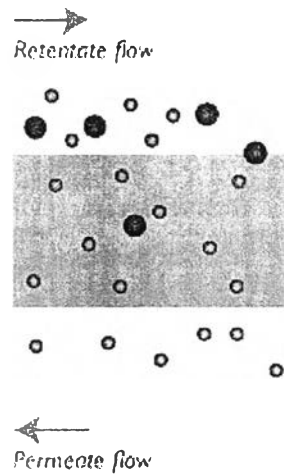


**Figure 2.2** The solution-diffusion mechanism for a nonporous membrane ([www.co2crc.com.au/aboutccs/cap membranes.html](http://www.co2crc.com.au/aboutccs/cap_membranes.html)).

The third type is called an asymmetric membrane (Figure 2.3). Asymmetric membrane denotes the structure consisting of a dense skin layer and a porous support layer. In the support layer, the polymer matrix and the pores are co-continuously connected across the layer. The three-dimensionally continuous polymer network exhibits the sufficient mechanical strength, and allows gases to pass through the three-dimensionally continuous pores without gas resistance.

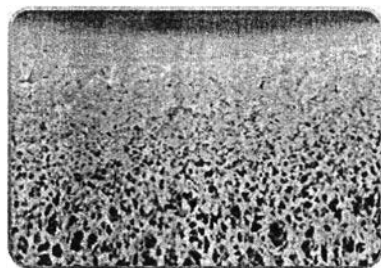


**Figure 2.3** Asymmetric membrane (<http://www.primewater.com>).

In polymeric membrane, the separation is based on a solution-diffusion mechanism, which involves molecular-scale interactions of the permeating molecule with the membrane polymer. The mechanism assumes that each molecule

of gas is adsorbed by the membrane at one interface, transported by diffusion across the membrane through the voids between the polymeric chains (or called free volume), and desorbed at the other interface. According to the solution-diffusion model, the permeation of molecules through membrane is controlled by two major parameters: the thermodynamic factors, called the solubility coefficient ( $S$ ) and a kinetic parameter, called the diffusivity coefficient ( $D$ ). Diffusivity is a measure of the mobility of individual molecules passing through the void between polymeric chains in a membrane material. The solubility coefficient equals the ratio of sorption uptake normalized by some measure of uptake potential, such as partial pressure. Solubility coefficient ( $S$ ) reflects the number of molecules dissolved in membrane material. Flux or permeability ( $P$ ) defined in Equation (2.1), represents the quantity of mass transport through the membrane.

$$P = D \times S \quad (2.1)$$

where the permeability ( $P$ ) is in Barrer ( $1 \text{ Barrer} = 10^{-10} \text{ cm}^3 \cdot (\text{STP}) \cdot \text{cm} / (\text{cm}^2 \cdot \text{s} \cdot \text{cm} \cdot \text{Hg}) = 3.34 \times 10^{-16} \text{ mol} \cdot \text{m} / (\text{m}^2 \cdot \text{s} \cdot \text{Pa})$ ), the solubility ( $S$ ) is in  $\text{cm}^3 \cdot (\text{STP}) / (\text{cm}^3 \cdot \text{bar})$ , and the diffusivity coefficient ( $D$ ) is in  $\text{cm}^2 / \text{s}$ .

The ability of a membrane to separate two gas molecules called membrane selectivity,  $\alpha_{A/B}$  which is an ideal separation factor, can describe the ability of a membrane to separate gaseous mixture of  $A$  and  $B$  and can be written in Equation (2.2) as a ratio of the permeability of component  $A$  and  $B$ .

$$\alpha_{A/B} = \frac{P_A}{P_B} \quad (2.2)$$

where  $P_A$  and  $P_B$  are the permeabilities of pure gases,  $A$  and  $B$  that pass through the membrane, respectively.

Since permeability depends on both diffusion coefficient ( $D$ ) which affected the mobility of each molecule in dense membrane, and solubility coefficient ( $S$ ) which reflected the number of molecules dissolved in membrane material, so membrane selectivity ( $\alpha_{A/B}$ ) can be written in Equation (2.3) as product of the diffusivity selectivity and solubility selectivity.

$$\alpha_{A/B} = \left( \frac{D_A}{D_B} \right) \left( \frac{S_A}{S_B} \right) \quad (2.3)$$

where  $D_A/D_B$  is the diffusivity selectivity and  $S_A/S_B$  is the solubility selectivity.

The diffusivity selectivity is based on the inherent ability of polymer matrix to function as size and shape selectivity media. This ability is determined by such factor as polymer segmental mobility, inter-segmental packing and the diameter of the component to be separated. The solubility selectivity, on the other hand, is determined by the difference of the condensabilities of the two penetrants as well as physical interaction of the penetrants with the particular polymer of which the membrane is composed (Suntiworawut, 2009).

Therefore, the difference in permeability is resulted not only from diffusivity (mobility) difference of the various gas species, but also from difference in the physicochemical interactions of these species with the polymer that determine the amount that can be accommodated per unit volume of the polymer matrix. The balance between the solubility selectivity and the diffusivity selectivity determines the selective transport of the component in a feed mixture (Chung *et al.*, 2007).

### 2.1.3 Mixed Matrix Membranes (MMMs)

Permeation models for mixed matrix membranes with porous particles are used to predict effective permeability of a gaseous penetrant in a mixed matrix membrane as functions of continuous phase (polymer matrix) permeability, dispersed phase (porous particles) permeability and volume fraction of dispersed phase.

Bouma *et al.* (1997) used Maxwell–Wagner–Sillar model given in Equation (2.4) to calculate the effective permeability of a mixed matrix membrane with a dilute dispersion of ellipsoids:

$$P_M = P_c \left[ \frac{nP_d + (1-n)P_c - (1-n)\phi_d(P_c - P_d)}{nP_d + (1-n)P_c + n\phi_d(P_c - P_d)} \right] \quad (2.4)$$

where  $P_M$  is effective permeability of a gaseous penetrant in a mixed matrix membrane,  $P_c$  is continuous phase permeability,  $P_d$  is dispersed phase permeability,  $\phi_d$  is volume fraction of dispersed phase and  $n$  is particles shape factor.

In this equation, the limit of  $n = 0$  leads to parallel two-layer model provided in Equation (2.5) and can be expressed as an arithmetic mean of the

dispersed and continuous phase permeabilities (Vu *et al.*, 2003 and Moore *et al.*, 2004).

$$P_M = \phi_d P_d + (1 - \phi_d) P_c \quad (2.5)$$

Moreover, when  $n = 1$  the Maxwell's model is simplified to series two-layer model shown in Equation (2.6).

$$\frac{1}{P_M} = \frac{\phi_d}{P_d} + \frac{\phi_c}{P_c} \quad (2.6)$$

where  $\phi_c = (1 - \phi_d)$

It is very important to mention that the minimum and maximum values of the effective permeability of a penetrant in a mixed matrix membrane can be given by the series and parallel two-layer models, respectively. The minimum value corresponds to a series model and the maximum value of  $P_M$  occurs when both phases are assumed to work in parallel to the flow direction (Gonzo *et al.*, 2006).

Under the random particle distribution condition, one can use the geometric mean model defined in Equation (2.7) to calculate effective permeability of a gas penetrant in a mixed matrix membranes:

$$P_M = P_c^{\phi_c} + P_d^{\phi_d} \quad (2.7)$$

In Equation (2.4), then  $n = 1/3$  corresponds to dilute suspension of spherical particles and leads to the following Equation (2.8) known as the Maxwell's Equation:

$$P_M = P_c \left[ \frac{P_d + 2P_c - 2\phi_d(P_c - P_d)}{P_d + 2P_c + \phi_d(P_c - P_d)} \right] \quad (2.8)$$

Maxwell's model is the most famous equation to predict the mixed matrix membrane permeability. Maxwell presented this equation in 1873, to predict the electrical conduction through a heterogeneous media. On the other hand, because the electrical conduction through a heterogeneous media is analogues with the flux through membranes, one can use Maxwell's model to predict permeability in the mixed matrix membranes (Bouma *et al.*, 1997). This well-known equation has been used by several researchers to calculate mixed matrix membrane permeability.

The Maxwell equation is applicable to a dilute suspension of spheres and can only be applicable for low loadings, when the volume fraction of filler particles is less than about 20 %, because of the assumption that the streamlines around particles are not affected by the presence of nearby particles. In addition, the Maxwell model cannot predict the permeability of mixed matrix membranes at the maximum packing volume fraction of filler particles. Furthermore, the Maxwell model does not account for particle size distribution, particle shape, and aggregation of particles.

To calculate the permeability of mixed matrix membrane with a high filler volume fraction, the so-called Bruggeman model defined in Equation (2.9), originally developed for the dielectric constant of particulate composites, can be used. This equation considers the effect of adding additional particles to a dilute suspension and for random dispersion of spherical particles, which leads to:

$$\left(\frac{P_M}{P_c}\right)^{-1/3} \left(\frac{(P_M/P_c) - (P_d/P_c)}{1 - (P_d/P_c)}\right) = 1 - \phi_d \quad (2.9)$$

Although Bruggeman model is applicable for high loadings, this equation, similar to that of the Maxwell model, cannot predict the permeability of mixed matrix membranes at the maximum packing volume fraction of filler particles. In addition, it does not account for particle size distribution, particle shape, and aggregation of particles. Furthermore, to estimate effective permeability by using this equation, a trial and error procedure is needed.

The Lewis–Nielsen model given in Equation (2.10), originally proposed for the elastic modulus of particulate composites, can be adapted to permeability as (Lewis *et al.*, 1997 and Nielsen, 1973):

$$P_M = P_c \left[ \frac{1 + 2(((P_d/P_c) - 1)/((P_d/P_c) + 2))\phi_d}{1 - (((P_d/P_c) - 1)/((P_d/P_c) + 2))\phi_d\psi} \right] \quad (2.10)$$

where  $\psi = 1 + \left(\frac{1 - \phi_m}{\phi_m^2}\right)\phi_d$  and  $\phi_m$  is the maximum packing volume fraction of filler particles, which is 0.64 for random close packing of uniform spheres. The Lewis–



Nielsen model may include the effects of morphology on permeability, because  $\phi_m$  is functions of particle size distribution, particle shape, and aggregation of particles.

Similar to Lewis–Nielsen model, the Pal model defined in Equation (2.11) can also be used to calculate the effective permeability of mixed matrix membranes with maximum packing volume fraction of filler particles and may include the effects of morphology on permeability through the parameter  $\phi_m$ . This equation is:

$$\left(\frac{P_M}{P_c}\right)^{1/3} \left(\frac{(P_d/P_c)-1}{(P_d/P_c)-(P_M/P_c)}\right) = \left(1 - \frac{\phi}{\phi_m}\right)^{-\phi_m} \quad (2.11)$$

However, the Pal model, like the Bruggeman model, is an implicit relationship that needs to solve numerically for  $P_M$ . On the other hand, according to the percolation theory, a simple power law can describe the relation between composite permeability and filler concentration near the percolation threshold (Gonzo *et al.*, 2006) as provided in Equation (2.12):

$$P_M = P_c(\phi_d - \phi_t)^t \quad (2.12)$$

where  $\phi_t$  is the percolation threshold (critical volume fraction of the filler) and  $t$  is the critical exponent.

Based on this theory, Chiew and Glandt (1983) presented an extension of Maxwell model in terms of  $\phi_d$ :

$$\frac{P_M}{P_c} \approx 1 + 3\beta\phi_d + 3(\beta\phi_d)^2 + O(\phi_d^3) \quad (2.13)$$

$\beta$  is defined as: 
$$\beta = \frac{P_d - P_c}{P_d + 2P_c}$$

where  $\beta$  is a convenient measure of penetrant permeability difference between the two phases and it is bounded by  $-0.5 \leq \beta \leq 1$ . Also,  $\beta = -0.5$  corresponds to totally non-permeable particle (e.g.  $P_d = 0.29$ ) and  $\beta = 1$  implies the perfectly permeable filler particle (disperse phase or  $P_c = 0$ ), while,  $\beta = 0$ , states the equal permeability in both phases.

In Equation (2.13), the second term represents the interaction between particles and continuous media and the third term implies the interaction between particles.

In addition, by taking the original Maxwell equation, Chiew and Glandt proposed an equation in terms of  $\phi_d$  as shown in Equation (2.14):

$$\frac{P_M}{P_c} = 1 + 3\beta\phi_d + K(\phi_d)^2 + O(\phi_d^3) \quad (2.14)$$

where  $K = a + b\phi_d^{1.5}$  and

$$a = -0.002254 - 0.123112\beta + 2.93656\beta^2 + 1.690\beta^3$$

$$b = 0.0039298 - 0.803494\beta - 2.16207\beta^2 + 6.48296\beta^3 + 5.27196\beta^4$$

It is obvious that when particle loading is low ( $\phi_d \ll 1$ ), term of order  $\phi_d^2$  and above is negligible in comparison with term of order  $\phi_d$  and Glandt equation gives the same results as Maxwell model. In other words, comparison of the Maxwell and the Glandt model indicates that, although the particle size was neglected in the Maxwell equation compared with the mean distance within the particles, the interaction between the particles and the continuous media is considered (Aroon *et al.*, 2010).

## 2.1.4 Effects of Environmental Conditions on Polymer Permeability

### 2.1.4.1 *Temperature Effects on Permeability*

The thermal effects on solubility and diffusion show opposite trends. Generally, for gas adsorption, solubility decreases with increases in temperature due to the condensability of the penetrant at lower temperatures. The solubility dependence with temperature is typically written in terms of the Van't Hoff relationship shown in Equation (2.15).

$$S = S_o \cdot \exp\left(-\frac{\Delta H_s}{R \cdot T}\right) \quad (2.15)$$

where  $S_o$  is a constant and  $\Delta H_s$  is the partial molar enthalpy of sorption. The solubility in thermodynamic terms is a two-step process. The first step involves the condensation of the gas molecule in a polymer, followed by creation of a molecular

scale gap for accommodating the gas molecule. These individual steps contribute to the total enthalpy of sorption and are mathematically represented in Equation (2.16):

$$\Delta H_s = \Delta H_{condensation} + \Delta H_{mixing} \quad (2.16)$$

For low molecular weight super critical gases, low condensability causes the mixing step to control the sorption property of a polymer. For weak interactions between the gas molecule and the polymer, the change in enthalpy of mixing is positive. This leads to an increase in solubility with an increase in temperature. For the case of condensable gases and vapors, the enthalpy change for condensation is negative and dominant, thereby showing decreasing solubility with increasing temperature.

Whereas the temperature dependence on gas diffusion is expressed in terms of an Arrhenius type relationship, as movement of gas molecules through a membrane is considered a thermally activated process. Mathematically, the temperature dependence of diffusion is given in Equation (2.17):

$$D = D_o \cdot \exp\left(\frac{\Delta E_D}{R \cdot T}\right) \quad (2.17)$$

where  $D_o$  is the pre-exponential factor and  $E_D$  is the activation energy of diffusion. Studies on the thermal effects during gas transport have shown that the activation energy term is dependent on the size of the penetrant and not on its mass. Diffusion is the most temperature sensitive transport parameter, in comparison to solubility and permeability. Combining the temperature dependence equations for the diffusion and sorption coefficients, the temperature effect on gas permeability is given in Equation (2.18):

$$P = P_o \cdot \exp\left(\frac{\Delta E_p}{R \cdot T}\right) \quad (2.18)$$

where  $E_p$  is the activation energy of permeation and is an algebraic sum of  $E_D$  and  $\Delta H_s$ . In general, permeability increases with increasing temperature. However, there are exceptions, especially near the glass transition temperature of the polymer, where opposite trends have been observed. These observations were explained in terms of pressure effects on the polymer under isothermal operating conditions. The high

stress caused by the applied gas pressure was stated to cause a transition in the polymer from a rubbery state to a glassy state.

#### 2.1.4.2 Pressure and Concentration Effects on Permeability

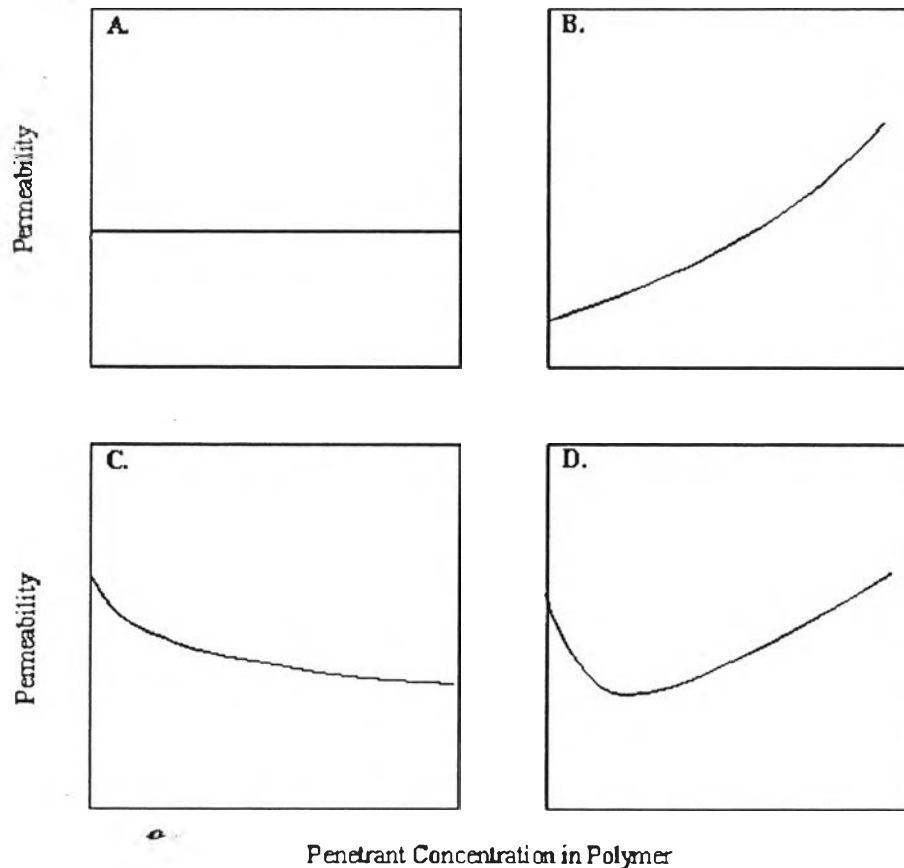


**Figure 2.4** Typical forms of permeability dependence on gas concentration during gas transport through polymer membranes (Koros *et al.*, 1987).

The effect of pressure and the gas concentration in the membrane is a major challenge in effective modeling of the gas transport process. Typical effects of gas pressure on permeability are shown in Figure 2.4.

The first response (response A) is for the ideal case as both diffusion and solubility are assumed independent of gas pressure. This type of behavior is observed for the case of supercritical gas permeation in amorphous polymers. The response B is characteristics of a gas plasticization effect on the

polymer and is observed during organic vapor permeation in rubbery polymers. Response C corresponds to the case of highly soluble gases in glassy polymer. The last response (D) is a combination of responses (B) and (C) and is observed in the case of permeation of organic vapors or plasticizing gas, such as CO<sub>2</sub>, in glassy polymers.

## 2.2. Literature Review

Gas separation through membranes has emerged as an important unit operation offering specific advantages over conventional separation methods such as cryogenic distillation and adsorption. Conventional membranes used for gas separation are classified as polymeric membranes, inorganic membranes, and mixed matrix membranes.

### 2.2.1 Polymeric Membranes

Polymeric membranes are currently the dominant materials for gas separation processes because they have the desired mechanical property and the flexibility to be processed into different modules. With regards to the separation of CO<sub>2</sub> from natural gas streams, these membranes selectively transmit CO<sub>2</sub> versus CH<sub>4</sub> (Shimekit and Mukhtar, 2012). The two types of polymeric membranes that are commercially available for gas separations are glassy and rubbery membranes. Glassy membranes are rigid and glass-like, and operate below their glass transition temperatures. On the other hand, rubbery membranes are flexible, soft and operate above their glass transition temperatures. Mostly, rubbery polymers show a high permeability, but a low selectivity, whereas glassy polymers exhibit a low permeability but a high selectivity. Glassy polymeric membranes dominate industrial membrane separations because of their high gas selectivities, along with good mechanical properties (Bastani *et al.*, 2013).

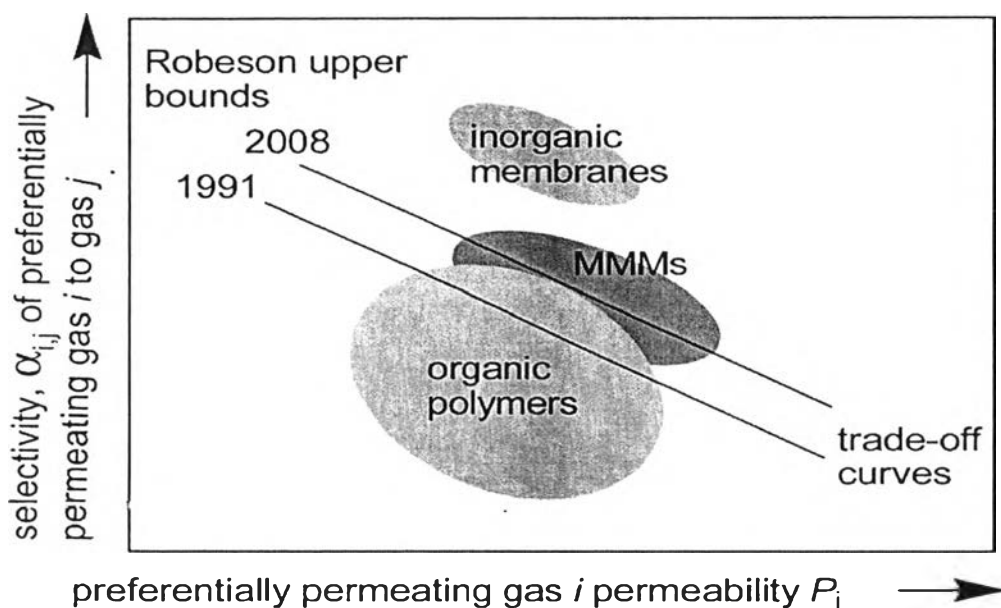


**Figure 2.5** Schematic presentation of the trade-off between permeability and selectivity with the 1991 and 2008 Robeson upper bounds (Robeson, 1991, 2008).

Generally, polymeric membranes have been known for their excellent intrinsic transport properties, high processability and their low cost. However, polymeric membranes are still ineffective in meeting the requirement for the current advanced membrane technology as these materials have demonstrated a trade-off between the permeability and selectivity (Figure 2.5), with an ‘upper-bound’ evident as proposed by Robeson (Goh *et al.*, 2011). Thus, the current research trend has focused on pushing the polymer performance above the upper bound and into the economically attractive region as showed by inorganic membranes.

### 2.2.2 Inorganic Membranes

Inorganic membranes are used for gas separation due to their superior thermal, mechanical and chemical stability, good erosion resistance, insensitivity to bacterial action and a long operational life (Caro *et al.*, 2000). Microporous and dense membranes are the two types of inorganic membranes that are suitable for high temperature gas separation applications. Dense, nonporous inorganic membranes are made of polycrystalline ceramic material, in particular made of perovskites,

palladium and its alloys, silver and nickel. Microporous inorganic membranes made of glass, metal, alumina, zirconia, zeolite and carbon membranes are commercially used as porous inorganic membranes. These membranes vary greatly in pore size, support material and configuration. A microporous ceramic membrane system generally consists of a macroporous ceramic support, some ceramic intermediate layers, and eventually a highly selective top layer. The support provides mechanical strength to the system. The intermediate layers bridge the gap between the large pores of the support and the small pores of the top layer. The top layer has separating capacities (Baker, 2004). Although inorganic membranes are more expensive than polymeric membranes, they possess advantages of temperature and wear resistance, well-defined stable pore structure, chemically inertness, and better selectivity than the polymeric membranes. However, due to the lack of technology to form continuous and defect-free membranes, high cost of production and handling issues e.g., brittleness, the commercial applications of inorganic membranes are still limited.

#### 2.2.2.1 Alumina Membranes

The generally mesoporous structure of alumina dictates that transport within membranes fabricated from it will take place by a Knudsen diffusion mechanism. Since selectivity in this regime is limited, and the rate of diffusion is controlled by molecular weight, alumina membranes are of limited use in the separation of gases. With mixtures such as CO<sub>2</sub>/N<sub>2</sub>, where the gases have similar mass, and CO<sub>2</sub>/H<sub>2</sub>, where selectivity toward the heavier component is required, alumina is undesirable as a membrane material. Alumina finds its use in the separation of gases mainly as a support, where its sound structural properties, and chemical and hydrothermal stabilities beyond 1,000 °C make it very desirable. A few attempts have been made to modify alumina membranes to facilitate CO<sub>2</sub> surface diffusion with limited success (Shekhawat *et al.*, 2003).

Uhlhorn *et al.* (1989) introduced magnesia into the  $\gamma$ -alumina membrane to enhance the adsorption and mobility of CO<sub>2</sub>. They modified a  $\gamma$ -alumina membrane system by impregnating magnesia to induce the surface diffusion of CO<sub>2</sub>. They reported that the introduction of magnesia into  $\gamma$ -alumina creates

stronger basic sites, which result in stronger bonding of CO<sub>2</sub> to the modified surface. Therefore, adsorption of CO<sub>2</sub> on the surface becomes partially irreversible. They concluded that the more strongly bonded CO<sub>2</sub> is less mobile, resulting in lower CO<sub>2</sub> permeability across the membrane.

Cho *et al.* (1995) also modified  $\gamma$ -alumina with CaO in an attempt to enhance CO<sub>2</sub>/N<sub>2</sub> separation by introducing interaction between CO<sub>2</sub> molecules and the pore wall. However, the CO<sub>2</sub>/N<sub>2</sub> separation factor was not different from the Knudsen diffusion mechanism. They also prepared silica-modified  $\gamma$ -alumina to improve the CO<sub>2</sub>/N<sub>2</sub> separation factor. The CO<sub>2</sub>/N<sub>2</sub> separation factor was 1.72 at 25 °C and decreased with increasing temperature. It was concluded that surface diffusion could be applied as a separation mechanism when the pore size is very small and the temperature is low.

#### 2.2.2.2 Zeolite Membranes

Zeolites are crystalline aluminosilicates with a uniform pore structure and a minimum channel diameter range of 0.3 to 1.0 nm. The presence of molecular-sized cavities and pores make the zeolites effective as shape-selective materials for a wide range of separation applications. These cavities are interconnected by pore openings through which molecules can pass. The electrical charge or polarity of the zeolites also functions to attract or sort molecules. This ability to selectively adsorb molecules by size and polarity is the key to the unusual efficiency of synthetic zeolites as the basis for separation. By tailoring the chemistry and structure of the materials used to prepare them, synthetic zeolites can be modified to provide a wide range of desired adsorption characteristics or selectivities and can be used as a membrane for gas separation applications.

Separation occurs in zeolite membranes by both molecular sieving and surface diffusion methods because the pore sizes of zeolite membranes are of molecular dimensions. In zeolite membranes, both molecular sizes relative to the zeolite pore, and the relative adsorption strengths determine the faster permeating species in a binary mixture (Shekhawat *et al.*, 2003).

Kusakabe *et al.* (1997) synthesized a Y-type zeolite membrane to determine the permeation properties for single-component, as well as



for the equimolar mixtures of gases. The CO<sub>2</sub> permeance was approximately the same for the single-component system and the mixed CO<sub>2</sub>/N<sub>2</sub> or CO<sub>2</sub>/CH<sub>4</sub> system. However, the N<sub>2</sub> or CH<sub>4</sub> permeances were significantly decreased for an equimolar feed at lower temperatures. This selective permeation was due to competitive adsorption of CO<sub>2</sub> molecules in micropores of the Y-type zeolite membrane. They concluded that the CO<sub>2</sub> molecules, adsorbed on the mouth of the micropores of the membrane, impeded the penetration of nonadsorptive molecules (N<sub>2</sub> or CH<sub>4</sub>) from entering into the pores. They also reported that the CO<sub>2</sub> and N<sub>2</sub> permeances increased initially due to water desorption from the membrane surface before it gradually decreased with time due to possible adsorption of impurities. Separation factors were obtained as high as 100 and 21 for CO<sub>2</sub>/N<sub>2</sub> and CO<sub>2</sub>/CH<sub>4</sub> mixtures, respectively, at 30 °C. They observed a decrease in separation factors and in permselectivities with increasing permeation temperatures.

#### 2.2.2.3. Carbon Membranes

Carbon membranes for gas separations are typically produced by the pyrolysis of thermosetting polymers. The pyrolysis temperature, typically in the range of 500 to 1,000 °C, depends upon the type of precursor material and dictates the separation performance of the carbon membranes (Shekhawat *et al.*, 2003). Pyrolysis of polymeric compounds leads to carbon material with a narrow pore size distribution below molecular dimensions ( $< 1$  nm), which makes it possible to separate gases with very similar molecular sizes. The predominant transport mechanism of most carbon membranes is molecular sieving. The selection of precursor polymer, the membrane preparation method, and the carbonization process determine the performance of carbon molecular sieve membranes. The mechanical stability can be improved by supporting a thin carbon membrane on a porous support material, such as  $\alpha$ -alumina. The high thermal and chemical stability of these membranes provide hope in gas separation applications, such as separation of CO<sub>2</sub> in flue gas emissions from power plants (Yang, *et al.*, 2008).

Yoshimune and Haraya (2013) investigated the permeation properties of single and binary CO<sub>2</sub>/CH<sub>4</sub> mixture using a module of carbon hollow fiber membranes derived from sulfonated poly (phenylene oxide) (SPPO). SPPO

carbon membrane module had a sharp pore-size distribution in the range of 0.35-0.4 nm, and showed high CO<sub>2</sub>/CH<sub>4</sub> ideal selectivity for both single and binary gas separation. The SPPO carbon membrane module achieved excellent gas separation performance, and the CO<sub>2</sub>/CH<sub>4</sub> ideal selectivity was 197 at 25 °C in the single gas system. They also studied that the effects of permeation temperature, total feed pressure and CO<sub>2</sub> concentration in the feed on separation performances of the carbon membrane module. They found that the CO<sub>2</sub>/CH<sub>4</sub> ideal selectivity decreased slightly with the increasing permeation temperature, total feed pressure, and CO<sub>2</sub> concentration in the feed.

### 2.2.3 Mixed Matrix Membranes (MMMs)

The investigation of MMMs for gas separation was first reported in 1970s with the discovery of a delayed diffusion time lag effect for CO<sub>2</sub> and CH<sub>4</sub> when adding 5A zeolite into rubbery polymer polydimethylsiloxane (Pechar *et al.*, 2006). Paul and Kemp found that the addition of 5A into the polymer matrix caused very large increases in the diffusion time lag but had only minor effects on the steady-state permeation. To enhance the commercial applicability of polymer membrane separation process, Kulprathipanja and coworkers at UOP LLC (1986 and 1988) developed the MMM that allows the membrane selectivity to be increased through gas solubility optimization (Singha-in, 2008). MMMs attract attention as a possibility to improve the permeability-selectivity properties of polymer membranes. Over the past decades, in order to establish MMM with higher gas separation performance relative to the neat polymeric and inorganic membranes, various inorganic materials have been explored and numerous have been identified as potential filler in membrane application. The most heavily researched type inorganic fillers are probably zeolite, CMSs and silica nano particles which have been traditionally incorporated into the polymer matrix (Goh *et al.*, 2011).

#### 2.2.3.1 *Zeolite as a Filler in Polymeric Matrix*

For the last few decades, the improvement in MMM performance using zeolite as the dispersed phase has resulted in the commercial alternative over the polymeric and inorganic membrane. The integration of

nanoporous molecular sieves such as zeolites into polymeric membranes has attracted much attention, since one can in principle combine the size and shape selectivity of nanoporous materials with the methodology and mechanical stability of polymers (Jeazet *et al.*, 2012).

Yong *et al.* (2001) prepared interfacial void-free Matrimid polyimide (PI) membranes filled with zeolites introducing 2,4,6-triaminopyrimidine (TAP). TAP enhanced the contact of zeolite particles with polyimide chains presumably by forming hydrogen bonding between them. It was observed that the amount of TAP to eliminate the interfacial void could be well related with the number of external hydroxyl groups of zeolites. The void-free PI/zeolite 13X/TAP membrane showed the higher gas permeability for He, N<sub>2</sub>, O<sub>2</sub>, CO<sub>2</sub> and CH<sub>4</sub> with a little expense of permselectivity compared with the PI/TAP membrane, while the PI/zeolite 4A/TAP membrane showed the lower permeability but higher permselectivity.

Husain and Koros (2007) fabricated mixed matrix asymmetric hollow fiber membrane by spinning via a dry jet-wet quench procedure, incorporating surface modified inorganic small pore size zeolites into an Ultem<sup>®</sup> 1000 polyetherimide matrix. Due to poor adhesion between the zeolites and the polymer phase, they modified zeolites via two separate techniques: Ultem sized and Grignard treated. The first method of increasing zeolite-polymer compatibility via the use of silane coupling agents and subsequent polymer “sizing” did not increase the selectivity of the mixed matrix membrane. On the other hand, hollow fiber asymmetric membranes incorporating Grignard reagent-modified zeolites demonstrated significant selectivity enhancement of 10 % for O<sub>2</sub>/N<sub>2</sub>, 29 % for He/N<sub>2</sub>, 17 % for CO<sub>2</sub>/CH<sub>4</sub> pure gases and 25 % for mixed gas CO<sub>2</sub>/CH<sub>4</sub> pairs over neat polymer results.

Ahmad and Hägg (2013) prepared 4A/Matrimid mixed matrix membranes to investigate the effect of zeolite 4A loading, operating temperature, feed pressure and membrane annealing temperature on the separation properties of N<sub>2</sub>, H<sub>2</sub>, O<sub>2</sub> and CO<sub>2</sub> in single gas permeation. They observed that zeolite 4A particles up to 20 wt.% were homogeneously dispersed and adhered within the

polymer without aggregation. However the loading of zeolite 4A was increased, permeability of the membranes increased for all the four gases  $N_2$ ,  $O_2$ ,  $H_2$  and  $CO_2$  with a corresponding decrease in their selectivity over  $N_2$ . So they annealed MMMs at higher temperature of  $250\text{ }^\circ\text{C}$  for 3 h and the annealing of MMMs had a positive effect on the gas separation properties that were improved compared to the MMMs without annealing. As the operating temperature was increased from  $30\text{ }^\circ\text{C}$  to  $70\text{ }^\circ\text{C}$ , permeability of all the gases increased such that  $N_2$  by 632 % which was the highest increase among the tested gases followed by  $O_2$  with a rise of 168 %,  $H_2$  by 162 % and the least increase was recorded for  $CO_2$  that was 62 %. The corresponding decrease in the selectivity of gas pairs  $O_2/N_2$ ,  $H_2/N_2$  and  $CO_2/N_2$  had been observed as 63 %, 64 % and 78 % respectively. They also found that feed pressure in the range of 2–8 bars had almost insignificant effect on the permeability and selectivity of 10 wt.% zeolite 4A/Matrimid annealed.

Junaidi *et al.* (2013) fabricated asymmetric SAPO-44 zeolite/polysulfone MMM with different loading (5-20 wt.%) to investigate the gas transport properties by using pure gas permeation tests of  $N_2$ ,  $CO_2$  and  $CH_4$  for each membrane. The authors reported that the most optimum sample was the membrane with 5 wt.% of SAPO-44 loading, which exhibited improved  $CO_2/N_2$  and  $CO_2/CH_4$  selectivities of 22 and 25, respectively, compared to other samples. However higher zeolite loadings (10 wt.% and above), the gas permeation properties of the MMMs were severely disturbed by the massive formation of large interfacial voids across the membrane surface due to the particle agglomeration. They concluded that modification on SAPO-44 filler and PSf matrix is required in order to embed high loading of SAPO-44 with defect-free MMMs and improve  $CH_4$  refining performance.

Peydayesh *et al.* (2013) prepared different SAPO-34 zeolites (2, 5, 10, 15, 20 wt.%) loaded Matrimid<sup>®</sup> 5218 mixed matrix membranes (MMM) by solution casting method. They observed that  $CO_2$  permeability increases as SAPO-34 loading increases, while that of  $CH_4$  decreases. The smaller gas molecules of  $CO_2$  can penetrate easier through the pores of SAPO-34 zeolite than the bigger  $CH_4$  molecules, the aim of selecting SAPO-34 as filler, and accordingly  $CO_2$  permeation increases, while that of  $CH_4$  decreases. The best separation performance

of the MMMs was achieved at the highest SAPO-34 zeolite loading of 20 wt.% as 97 % and 55 % increment for ideal selectivity and CO<sub>2</sub> permeability, respectively. Although the separation performance of the prepared SAPO-34/ Matrimid<sup>®</sup> 5218 MMMs is still under the Robeson's upper bound limit, they confirmed that the better selection of SAPO-34 zeolite as filler due to the improvement of the CO<sub>2</sub>/CH<sub>4</sub> separation performance.

Junaidi *et al.* (2014) fabricated asymmetric polysulfone MMMs incorporated with SAPO-34 zeolite as a framework of 0.38 nm pore size in different loading (5-30 wt.%) to investigate the gas transport properties by using pure gas permeation tests of N<sub>2</sub>, CO<sub>2</sub> and CH<sub>4</sub> for each membrane. They observed that well dispersion of SAPO-34 particles in the polymer matrix was less than 10 wt.% zeolite loading and the maximum CO<sub>2</sub> permeance (314.02 GPU) was achieved by incorporating 10 wt.% of SAPO-34 into asymmetric PSf membrane, resulting in the highest CO<sub>2</sub>/N<sub>2</sub> and CO<sub>2</sub>/CH<sub>4</sub> selectivities up to 26.1 and 28.2, respectively. According to the SEM images, the SAPO-34 aggregates formed in the 20 wt.% SAPO-34 zeolite/PSf MMM and disturbed the dense layer surface structure by generating large interfacial voids and as a result the CH<sub>4</sub> permeance was increased to 25.73 GPU while the CO<sub>2</sub>/CH<sub>4</sub> selectivity decreased by 37 %.

Most MMMs were reported to suffer from poor interaction between zeolite particles and polymer chains which may cause non-selective voids at the polymer-zeolite interface, polymer chain rigidification and pore blockage by the polymer chains and be the reasons for insufficient improvement of membrane performance. In addition, zeolite particles encounter the problem of formation of aggregates creating defects, especially if the polymer matrix is a glassy polymer. Poor adhesion at the zeolite-polymer interface can result in "sieve-in-a-cage" morphology that is responsible for the non-selective penetration of gas molecules, hence reduces the apparent selectivity of the mixed matrix membrane and increases the permeability (Verweij, 2012). Different methods to eliminate the voids, especially for glassy polymers are modification of the zeolite by a silane coupling agent, introducing low molecular weight materials, annealing the membrane above the T<sub>g</sub> of the polymer, and priming the surface of zeolites by polymer (Bastani *et al.*, 2013).

### 2.2.3.2 Carbon Molecular Sieve and Activated Carbon as Fillers in Polymeric Matrix

Vu *et al.* (2003) incorporated carbon molecular sieves (CMSs) into two different polymer matrices (Matrimid<sup>®</sup> 5218 and Ultem<sup>®</sup> 1000) to form mixed matrix membrane films for both the O<sub>2</sub>/N<sub>2</sub> and CO<sub>2</sub>/CH<sub>4</sub> separations. Mixed matrix films comprising high CMS particle loadings (up to 35 wt.%) dispersed within two polymer matrices were successfully formed from flat-sheet solution casting. They found out that the CMS membrane pyrolyzed to 800 °C for 2 h (CMS 800-2) was a good candidate for incorporation into mixed matrix membranes because it offered the highest CO<sub>2</sub>/CH<sub>4</sub> selectivity of 200 with a CO<sub>2</sub> permeability of 44 Barrer and an O<sub>2</sub>/N<sub>2</sub> selectivity of 13.3 with an O<sub>2</sub> permeability of 24 Barrer at 35 °C. Pure gas permeation test in CMS-Ultem and CMS-Matrimid mixed matrix membranes, showed enhancements by up to 40-45 %, respectively in CO<sub>2</sub>/CH<sub>4</sub> selectivity over the intrinsic selectivity of the pure Ultem<sup>®</sup> and Matrimid<sup>®</sup> polymer matrices. They confirmed that the effective permeabilities of the fast-gas penetrants (O<sub>2</sub> and CO<sub>2</sub>) through the mixed matrix membranes were also significantly enhanced over the intrinsic permeabilities of the Ultem<sup>®</sup> and Matrimid<sup>®</sup> polymer matrices. These CMS mixed matrix membranes exhibited excellent polymer-filler contact and a remarkable higher performance compared with those of the intrinsic polymer matrix.

Anson *et al.* (2004) fabricated two different activated carbons (AC): a powder with high surface area (AC1, 21.7 Å) and a commercial active carbon (AC2, 28.2 Å) into acrylonitrile-butadiene-styrene (ABS) copolymer. They analyzed the effect of temperature and pressure on the permeation rates of CO<sub>2</sub> and CH<sub>4</sub> and selective properties of the AC-ABS composite membranes in the range 20-50 °C, and in the feed pressure range from 2 to 8 atm. The AC-ABS membranes showed a simultaneous increase of CO<sub>2</sub> gas permeabilities (40-600 %) and CO<sub>2</sub>/CH<sub>4</sub> selectivities (40-100 %) over the intrinsic ABS permselectivity by increasing the percentage of carbon loaded in the mixed matrix composite membrane. They observed that AC1 is 3-3.5 more selective for CO<sub>2</sub> adsorption than CH<sub>4</sub>, whereas AC2 is 1.6-2.7 times more selective. They concluded that the increasing selectivities

with increasing AC content could not be due to a molecular sieving mechanism since the mean pore size of both dispersed phases (21.7 and 28.2 Å) are bigger than the molecular diameters of the permeate gases ( $d(\text{CO}_2)=3.3$  Å and  $d(\text{CH}_4)=3.9$  Å) and these results could be partially explained considering the existence of a surface flux through the micro-mesoporous carbon media, with a mechanism of preferential surface diffusion of  $\text{CO}_2$  (more adsorbable gas) over the  $\text{CH}_4$  gas (less adsorbable).

### 2.2.3.3 Metal Organic Frameworks (MOFs) as a Filler in Polymeric Matrix

The first patent on MOF-MMMs (Liu *et al.*, 2009) is that up to 20 wt.% of IRMOF-1 ( $\text{Zn}_4\text{O}(\text{R}_1\text{-BDC})_3$ ) particles were dispersed in Matrimid<sup>®</sup> polyimide and Ultem<sup>®</sup> polyetherimide. Single gas permeation measurements showed the improvements in  $\text{CO}_2$  and  $\text{H}_2$  gas permeabilities compared to the pure polymers without significant decrease in the corresponding ideal selectivities. The permeability of  $\text{CO}_2$  in 10 wt.% IRMOF-1/Ultem 1000 MMM increased 44 % without a significant decrease in the selectivity of  $\text{CO}_2/\text{CH}_4$  compared to the pure Ultem.

Zhang *et al.* (2008) prepared and incorporated a microporous metal-organic framework Cu-4,4'-bipyridine-hexafluorosilicate (Cu-BPY-HFS) to Matrimid<sup>®</sup> polymer to form free standing films. The permeability properties of Cu-BPY-HFS-Matrimid<sup>®</sup> mixed-matrix membranes were tested for the pure gases  $\text{H}_2$ ,  $\text{N}_2$ ,  $\text{O}_2$ ,  $\text{CH}_4$ , and  $\text{CO}_2$  and the gas mixtures  $\text{CO}_2/\text{CH}_4$ ,  $\text{H}_2/\text{CO}_2$  and  $\text{CH}_4/\text{N}_2$ . The ideal selectivity of  $\text{CH}_4/\text{N}_2$  increased from 0.95 to 1.21, which suggests that Cu-BPY-HFS has a strong affinity towards  $\text{CH}_4$  and favors its permeation. The Cu-BPY-HFS's affinity towards  $\text{CH}_4$ , and its large surface area increased the solubility of  $\text{CH}_4$  in the mixed-matrix membranes, which led to higher selectivity towards  $\text{CH}_4$ .

Perez *et al.* (2009) used MOF-5 in Matrimid and found that permeability increased with the addition of MOF, but selectivity showed a different trend. Gas mixtures ( $\text{CO}_2/\text{CH}_4$ ,  $\text{N}_2/\text{CH}_4$ ) showed a marked increase in selectivity for  $\text{CH}_4$  due to the larger solubility of  $\text{CO}_2$  and  $\text{N}_2$  in the polymer matrix. This difference in solubility makes  $\text{CH}_4$  transport mostly diffusivity dependent and facilitated by the MOF-5 porosity as well as by the uniformity of the surface of its walls.  $\text{H}_2$  selectivity remained constant under all gas feed conditions tested.

Adams *et al.* (2010) studied a CuTPA (Cu and terephthalic acid)/PVA (poly vinyl acetate) mixed matrix membrane for gas separation. Their membranes performance was increased by adding 15 wt.% CuTPA. Although permeability decreased compared to pure polymeric membrane, selectivity increased significantly.

Ordonez *et al.* (2010) investigated the effect of ZIF-8 loading in Matrimid. The ZIF-8/Matrimid<sup>®</sup> MMMs permeability properties were tested for H<sub>2</sub>, CO<sub>2</sub>, O<sub>2</sub>, N<sub>2</sub>, CH<sub>4</sub>, C<sub>3</sub>H<sub>8</sub>, and gas mixtures of H<sub>2</sub>/CO<sub>2</sub> and CO<sub>2</sub>/CH<sub>4</sub>. Their results showed enhancement of permeability for up to 40 wt.% loading; above this, permeability decreased because of the transition from a polymer-driven to a MOF-controlled gas transport process. However, the selectivity growth was observed at higher MOF loadings.

Dai *et al.* (2012) reported the first successful production of dual layer asymmetric hollow fiber mixed matrix membranes containing ZIF-8 fillers into Ultem matrix to improve separation performance of the CO<sub>2</sub>/N<sub>2</sub> gas pairs. Their hybrid fibers showed increased permeance with permselectivity enhancements as high as 20 % over pure polymer and mixed gas measurements revealed promising permselectivity (as high as 32) in the hybrid membranes.

Basu *et al.* (2010) studied asymmetric Cu<sub>3</sub>(BTC)<sub>2</sub> containing MMMs based on Matrimid and Matrimid/Polysulphone blends for the separation of CO<sub>2</sub>/CH<sub>4</sub> and CO<sub>2</sub>/N<sub>2</sub> binary gas mixtures under different CO<sub>2</sub> feed composition and as a function of filler loading. Their results showed excellent compatibility between the two phases. Permeability of membranes increased as the percentage of MOF in the polymer increased. Moreover, selectivity of pair gases (CO<sub>2</sub>/CH<sub>4</sub> and CO<sub>2</sub>/N<sub>2</sub>) increased with increase in MOF percent for all polymeric matrixes. They attributed the growth of permeability to MOF porosity and enhancement of polymer d-spacing.

Bae *et al.* (2010) reported the outstanding performance of ZIF-90/6FDA-DAM MMMs, demonstrating that the combination of a selective, functionalized, MOF with a properly chosen high flux polymer. They incorporated ZIF-90 to three different poly(imide)s: Ultem, Matrimid, and 6FDA-DAM for fabricating a high performance gas separation membrane containing a MOF material.



On the other hand, Ultem and Matrimid mixed matrix membranes showed significantly enhanced CO<sub>2</sub> permeability without any loss of CO<sub>2</sub>/CH<sub>4</sub> selectivity. The performance of ZIF-90/6FDA-DAM mixed-matrix membranes clearly transcends the polymer upper bound for polymeric membrane performance drawn in 1991, and reaches the technologically attractive region. ZIF-90/6FDA-DAM membranes have unprecedented high performance for CO<sub>2</sub>/CH<sub>4</sub> separation and promising CO<sub>2</sub>/N<sub>2</sub> separation properties. The CO<sub>2</sub>/CH<sub>4</sub> mixed-gas selectivity of the ZIF-90 mixed-matrix membrane was even higher than the ideal selectivity measured by pure gas permeation, presumably because of selective sorption and diffusion of CO<sub>2</sub> in the ZIF-90 crystals.

Dorosti *et al.* (2014) fabricated MIL-53/Matrimid mixed matrix membranes with different MOF weight percentages (0, 5, 10, 15, and 20) wt.% for gas separation properties. CH<sub>4</sub> permeability of membranes increased slightly as the percentage of loading increased. The CO<sub>2</sub> permeability of membranes increased from 6.4 Barrer for pure Matrimid to 12.43 Barrer for 15 wt.% loading MOF. This significant enhancement can be explained by the breathing property of the MIL-53 pores in the presence of CO<sub>2</sub> molecules. The pore structure changed between the closed and open forms. CO<sub>2</sub> permeability showed that there was a 94 % increase in permeability compared to pure Matrimid for 15 wt.% MMMs. CO<sub>2</sub>/CH<sub>4</sub> selectivity also increased as MOF loading increased.

Duan *et al.* (2014) incorporated different MOF loadings: 10 wt.%, 20 wt.%, 30 wt.%, 35 wt.% and 40 wt.% Cu<sub>3</sub>(BTC)<sub>2</sub> into a model polymer (Ultem<sup>®</sup> 1000) using N,N-dimethyl acetamide as a solvent. Their results showed that there was no interfacial defects in the prepared MMMs when Cu<sub>3</sub>(BTC)<sub>2</sub> loading was less than 35 wt.%. Pure gas permeation tests showed that gas permeability increased obviously with Cu<sub>3</sub>(BTC)<sub>2</sub> loading increased, while ideal selectivities of CO<sub>2</sub>/N<sub>2</sub> and CO<sub>2</sub>/CH<sub>4</sub> were almost unchanged. For MMM with the best separation property, CO<sub>2</sub> permeability increased about 2.6 times and CO<sub>2</sub>/N<sub>2</sub> selectivity remained almost unchanged.